Multiple Transitions in Rotating Turbulent Rayleigh-Bénard Convection

Ping Wei, Stephan Weiss, and Guenter Ahlers

Phys. Rev. Lett. **114**, 114506 — Published 20 March 2015

DOI: 10.1103/PhysRevLett.114.114506

Multiple transitions in rotating turbulent Rayleigh-Bénard convection

Ping Wei[1], Stephan Weiss[1,2], and Guenter Ahlers[1]
[1]*Department of Physics, University of California, Santa Barbara, CA 93106, USA and*
[2]*Department of Physics, University of Michigan, Ann Arbor, MI 48109, USA*
(Dated: January 20, 2015)

Sometimes it is thought that sharp transitions between potentially different turbulent states should be washed out by the prevailing intense fluctuations and short coherence lengths and times. Contrary to this expectation, we found a *sequence* of such transitions in turbulent rotating Rayleigh-Bénard convection as the rotation rate was increased. This phenomenon was observed in cylindrical samples with aspect ratios (diameter/height) $\Gamma = 1.00$ and 0.50. It became most prominent at very large Rayleigh numbers up to 2×10^{12} where the fluctuations are extremely vigorous, and was manifested most clearly for $\Gamma = 1.00$. It was found in the heat transport as well as in the temperature gradient near the sample center. We conjecture that the transitions are between different large-scale structures which involve changes of symmetry and thus can not be gradual [1–3].

Turbulent flows involve large fluctuations and loss of coherence in space and time. Thus it was argued at times that Kolmogorov's theory of turbulence [4] implies that turbulent flows become featureless when the Reynolds number is large enough (for a discussion of this issue see for instance [5]). Apparently in contradiction to this expectation several experiments recently showed a sharp transition between two different turbulent states [5–9]. However, all of these investigations were carried out on systems with geometrical constraints in all physical directions, and it is not clear whether the sharp transitions are caused by boundary conditions or whether they would survive in the theoretically envisioned [4] unconstrained system. Indeed for one, namely turbulent rotating Rayleigh-Bénard convection, measurements were made as a function of the lateral extent (aspect ratio), and it was found that the observed transition moves toward zero rotation rate as the lateral system size approaches infinity [10, 11].

In this Letter we report that there is a *sequence* of sharp transitions in rotating turbulent Rayleigh-Bénard convection (RBC) which occurs with increasing rotation rate. They have been observed most clearly at very large Ra up to 2×10^{12} where fluctuations are extremely vigorous and coherence lengths are much smaller than the sample dimension. While the first transition may be attributed to the finite system size [10], it is unlikely that this explanation can be applied to the subsequent transitions.

Turbulent RBC occurs in a fluid confined between parallel horizontal plates heated from below [12–16]. Most of the temperature drop across the sample is sustained by two thin thermal boundary layers (BLs), one below the top and the other above the bottom plate [17–20]. The temperature throughout the bulk of the sample, even though vigorously fluctuating, remains nearly constant in the time average.

Rotating a sample of turbulent RBC about its vertical axis at an angular frequency Ω introduces a host of interesting new phenomena (see, for instance, [21]). The associated Coriolis force affects the velocity and temperature fields, and the heat transport as expressed in terms of the dimensionless Nusselt number Nu. Slow rotation at constant Ra leads to an *increase* of Nu [22] when Ra is not too large and the Prandtl number Pr is not too small. This phenomenon is due to Ekman pumping that occurs when thermal plumes that emerge from the thermal boundary layers are turned into vortices by the Coriolis force; these vortices pump hot or cold fluid from the bottom or top boundary layer into the bulk of the sample [8, 11, 22–29].

A remarkable experimental discovery was that Ekman pumping does not occur immediately when rotation starts. Rather, at a critical dimensionless rotation rate $1/\mathrm{Ro}_c$ (Ro is the Rossby number, proportional to $1/\Omega$) a sharp transition occurs where Ekman pumping sets in [8]. The value for $1/\mathrm{Ro}_c$ is proportional to $1/\Gamma$ where $\Gamma \equiv D/L$ with D the diameter and L the height of a cylindrical sample, showing that the laterally unbounded system has no transition [10, 11].

In view of the above discussion, it came as a surprise to us that the transition at $1/\mathrm{Ro}_c$ is not the only one in this system. For a fluid with $\mathrm{Pr} = 12.3$ and larger Ra values than had been used before to study $1/\mathrm{Ro}_c$ we found two additional sharp transition, to be labeled $1/\mathrm{Ro}_{c,2}$ and $1/\mathrm{Ro}_{c,3}$, which for $\mathrm{Ra} \simeq 10^{11}$ and $\Gamma = 1.00$ for instance (where $1/\mathrm{Ro}_c \simeq 0.25$) occurred roughly at $2/\mathrm{Ro}_c$ and $6/\mathrm{Ro}_c$. These transitions were found in the data for Nu, as well as in measurements of the vertical temperature gradient near the sample center. The detailed origin of these transitions between turbulent states is not known to us, but we presume that it involves a sudden change of large-scale structures of the turbulent flow. Although off hand it seems surprising that a sharp bifurcation should exist in this highly-fluctuating turbulent state with Ra as large as 2×10^{12}, changes of large-scale structures involve symmetry changes which can not occur gradually [1–3].

Experiments on thermal convection often are done in cylindrical vessels of diameter D and height L confined by a warm plate of temperature T_b from below and a

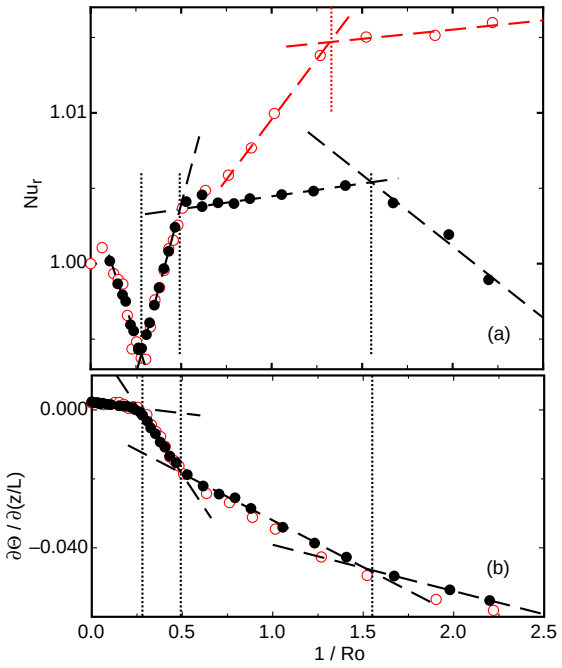

FIG. 1. (a): Nu_r, and (b): the temperature gradient at the sample center, both as a function of 1/Ro. Here and in subsequent figures the dashed lines are straight-line fits to various segments of data, and serve as guides to the eye. Black vertical dotted lines, from left to right: the location of $1/Ro_c = 0.280$, $1/Ro_{c2} = 0.492$, and $1/Ro_{c,3} \simeq 1.55$ respectively. Solid black circles: $Ra = 2.07 \times 10^{11}$(Nu(0) = 344). Open red circles: $Ra = 1.00 \times 10^{11}$(Nu(0) = 273).

colder plate at temperature T_t from above. The Rayleigh number $Ra = \alpha g \Delta T L^3/\nu\kappa$ and the Prandtl number $Pr = \nu/\kappa$ characterize this system. Here α, κ and ν denote the isobaric thermal expansion coefficient, the thermal diffusivity, and the kinematic viscosity of the fluid. These properties are evaluated at the mean temperature $T_m = (T_b+T_t)/2$. The gravitational acceleration is g, and $\Delta T \equiv T_b - T_t$. The angular rotation frequency Ω is expressed by the Rossby number $Ro = \sqrt{\alpha g \Delta T/L}/2\Omega$. We shall use 1/Ro because it is proportional to Ω. The Nusselt number is given by $Nu = QL/A\lambda\Delta T$. We shall give the relative Nusselt number $Nu_r = Nu(1/Ro)/Nu(0)$.

The apparatus was described before [30–32]. We used cylindrical samples with $L = D$ ($\Gamma = 1.00$) and $L = 2.00D$ ($\Gamma = 0.50$), where $D = 19.0$ cm. The fluid was a fluorocarbon C_6F_{14} (3M Fluorinert^{TM} FC72) with $Pr = 12.3$ and $T_m = 25°C$. The side walls were made of Lexan. The top and bottom plates of the cell were made of copper. The rotating table and the corresponding outer frame were as described in detail in an earlier publication [30]. We held Ra and Pr constant while measuring Nu for several different Ω. We also determined time-averaged temperatures near the center of the sample, as described in Ref. [32].

Figure 1(a) displays results for Nu_r as a function of

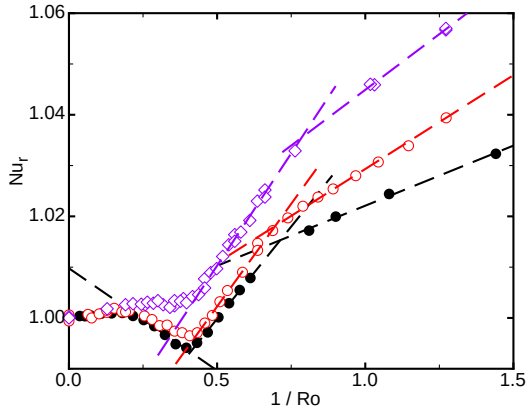

FIG. 2. The reduced Nusselt numbers Nu_r as a function of 1/Ro for water ($Pr = 4.38$), $\Gamma = 1.00$, $Ra = 2.3 \times 10^9$ (open purple diamonds), $Ra = 9.0 \times 10^9$ (open red circles), and $Ra = 1.8 \times 10^{10}$ (solid circles). Based on data from Ref. [30].

1/Ro. They are for $\Gamma = 1.00$, with $Ra = 2.07 \times 10^{11}$ (solid black circles) and 1.00×10^{11} (red open circles), and extend by a decade to larger Ra than had preciously been explored for $3 \lesssim Pr \lesssim 6$ [30]. Initially Nu_r decreased with increasing 1/Ro. This decrease occurs only at large Ra, and to our knowledge it has not been explained. Nu_r reached a minimum at $1/Ro_c \simeq 0.280$. For $1/Ro > 1/Ro_c$ Nu_r initially increased linearly with 1/Ro due to Ekman pumping. Within the resolution of the data Nu_r is independent of Ra over this range of 1/Ro.

A remarkable and unexpected new feature of the data is that $Nu_r(1/Ro)$ showed a second sharp transition at $1/Ro_{c,2} \simeq 0.492$ where the slope of Nu_r decreased abruptly while no discontinuity of Nu_r was resolved. For $1/Ro > 1/Ro_{c,2}$ Nu_r depended on Ra, being smaller for larger Ra. Yet another transition, with a discontinuous change in slope, is indicated by the data near $1/Ro_{c,3} \simeq 1.55$ for $Ra = 2.07 \times 10^{11}$ and near $1/Ro_{c,3} \simeq 1.33$ for $Ra = 1.00 \times 10^{11}$.

Figure 1(b) shows data for the dimensionless vertical temperature gradient $\partial\Theta/\partial(z/L)$ near the sample center. Here $\Theta \equiv (\langle T\rangle - T_m)/\Delta T$, $\langle ...\rangle$ indicates a time average, and z is the vertical coordinate. This local parameter also shows the three transitions, although the one at $1/Ro_{c,3}$ is not as well defined particularly at the smaller Ra.

Our observation of a sequence of transitions suggested a re-examination of earlier measurements. Some of those data are shown in Fig. 2. There one sees that those results are also consistent with both the transition at $1/Ro_c$ and a second transition at $1/Ro_{c,2}$. Figure 3 shows that evidence also for the third transition at $1/Ro_{c,3}$ can be found.

In Fig. 4 we show all transition points that we were able to identify for $\Gamma = 1.00$, both in the new measurements for $Pr = 12.3$ and in the older ones for $3.62 \leq Pr \leq 6.26$, as a function of Ra. One sees that the phenomenon of

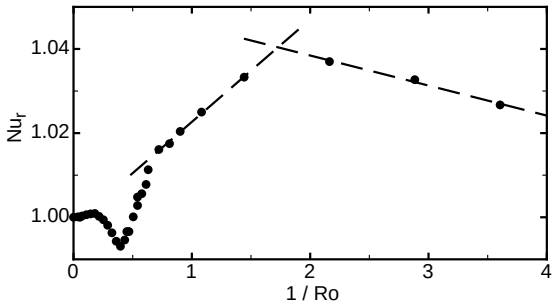

FIG. 3. An example of the reduced Nusselt number Nu_r as a function of 1/Ro for water over a wider range of 1/Ro than in Fig. 2. For this case Pr = 4.38 and $\mathrm{Ra} = 1.8 \times 10^{10}$. Based on data from Ref. [30].

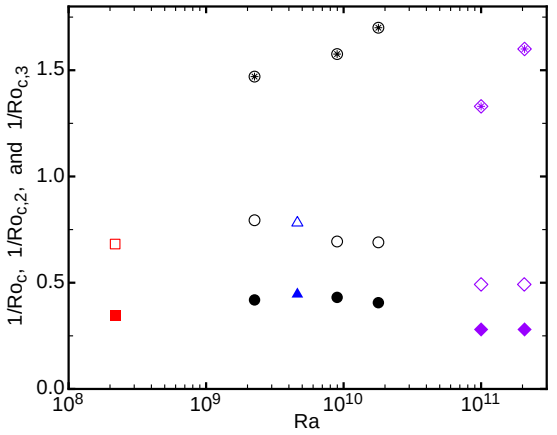

FIG. 4. Results for $1/\mathrm{Ro}_c$ (solid symbols), $1/\mathrm{Ro}_{c,2}$ (open symbols), and $1/\mathrm{Ro}_{c,3}$ (open symbols with stars) as a function of Ra. Blue triangles: Pr = 3.62. Black circles: Pr = 4.38. Red squares: Pr = 6.26. Purple diamonds: Pr = 12.3.

multiple transitions is not limited to large Ra, although there it becomes more obvious in the data as can be seen in Fig. 1 for $\mathrm{Ra} = 2.07 \times 10^{11}$.

Turning now to $\Gamma = 0.50$, we show in Fig. 5 new measurements of Nu_r as a function of 1/Ro for Pr = 12.3. Qualitatively, the results are consistent with those of Ref. [33] where for instance a reduction of Nu_r to about 0.966 was found for $\mathrm{Ra} = 4.3 \times 10^{15}$, Pr = 5.9, and 1/Ro = 2; but the data of Ref. [33] did not identify any transitions. In Fig. 5 one finds $1/\mathrm{Ro}_c = 0.612$ which, consistent with previous work [10], is slightly larger than twice the value $1/\mathrm{Ro}_c = 0.280$ found for $\Gamma = 1.00$ (see Fig. 1). For $\mathrm{Ra} = 8.0 \times 10^{11}$ a second transition at $1/\mathrm{Ro}_{c,2} = 2.10$ is found, but for $\mathrm{Ra} = 1.66 \times 10^{12}$ there is no evidence for a second sharp transition over the 1/Ro range covered by those data.

Also for $\Gamma = 0.50$ it is worth re-examining data published before. Thus, in Fig. 6 we show results from Ref. [11] for Pr = 4.38 and $\mathrm{Ra} = 2.3 \times 10^9$ which extend to rather large values of 1/Ro and which were thought

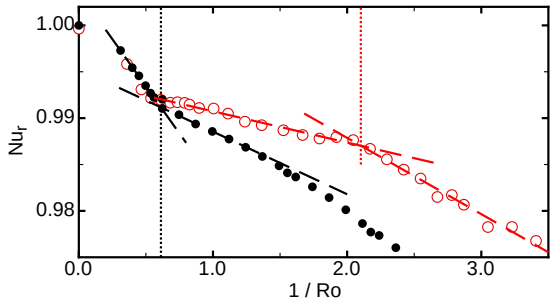

FIG. 5. The reduced Nusselt number Nu_r as a function of 1/Ro for $\Gamma = 0.50$, Pr = 12.3, $\mathrm{Ra} = 1.66 \times 10^{12}$ (solid black circles, Nu(0) = 680), and $\mathrm{Ra} = 8.0 \times 10^{11}$ (open red circles, Nu(0) = 540). The vertical dotted lines indicate the locations of $1/\mathrm{Ro}_c = 0.612$ and $1/\mathrm{Ro}_{c,2} = 2.10$.

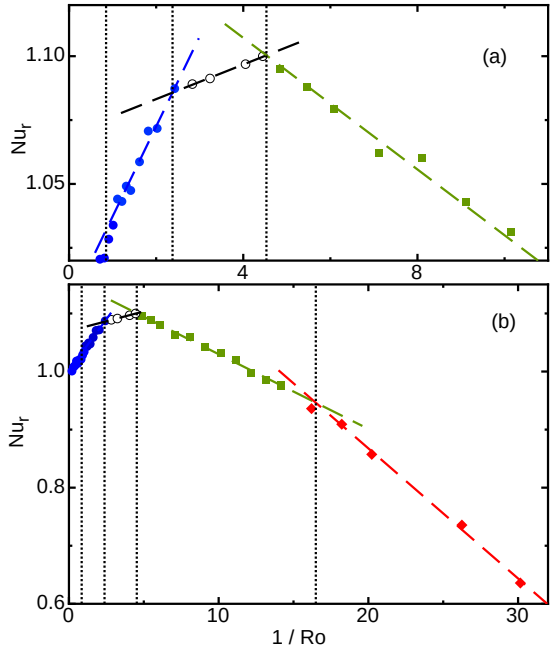

FIG. 6. The reduced Nusselt number Nu_r as a function of 1/Ro on two different scales for $\Gamma = 0.50$, Pr = 4.38, and $\mathrm{Ra} = 2.3 \times 10^9$. The vertical dotted lines, from left to right, indicate the location of $1/\mathrm{Ro}_c = 0.85$, $1/\mathrm{Ro}_{c2} = 2.38$, $1/\mathrm{Ro}_{c3} = 4.53$, and $1/\mathrm{Ro}_{c4} = 16.5$. The data are from Ref. [11].

to vary smoothly with 1/Ro for $1/\mathrm{Ro} > 1/\mathrm{Ro}_c \simeq 0.85$. While $1/\mathrm{Ro}_c$ is not resolved in this figure, evidence for three transitions at $1/\mathrm{Ro}_{c,2} = 2.38$, $1/\mathrm{Ro}_{c,3} = 4.53$, and $1/\mathrm{Ro}_{c,4} = 16.5$ can be found. We note that the result for $1/\mathrm{Ro}_{c,2}$ is consistent with the result $1/\mathrm{Ro}_{c,2} = 2.10$ for Pr = 12.3 displayed in Fig. 5.

In this Letter we presented new measurements of the heat transport by and the temperature gradient in the center of turbulent convection in the presence of rotation for samples of aspect ratios 1.00 and 0.50. We reached values of Ra up to 2×10^{12} at a Prantl number Pr = 12.3.

It was known from previous measurements that

$\mathrm{Nu}_r(1/\mathrm{Ro})$ undergoes a sharp transition at a value of $1/\mathrm{Ro} = 1/\mathrm{Ro}_c$ that depends on Pr (but apparently not on Ra) and in all cases studied was well below 1; but it was thought that for $1/\mathrm{Ro} > 1/\mathrm{Ro}_c$ $\mathrm{Nu}_r(1/\mathrm{Ro})$ varied smoothly with 1/Ro without any further singularities [21]. The new data show that actually there is a sequence of transitions, and that to a good approximation $\mathrm{Nu}_r(1/\mathrm{Ro})$ between successive transitions is well represented by straight lines. We confirm this finding by a close examination of previous measurements which had been interpreted as representing a smoothly varying $\mathrm{Nu}_r(1/\mathrm{Ro})$, but which upon closer examination also reveal sequences of several transitions.

While the observations presented in this Letter are contrary to the common belief that intense turbulent fluctuations would round out any transitions between different states that potentially could occur as Ra or 1/Ro is increased, they are consistent with the idea that the transitions are between different large-scale structures of different symmetries. As enunciated by L.D. Landau [1–3], symmetry-breaking transitions can not be gradual, and instead lead to sharp, albeit possibly continuous, transitions. This is in no way altered by the presence of fluctuations; for if it were, then there also would be no continuous phase transitions (*i.e.* critical points) in equilibrium systems.

The task ahead, of course, is to identify the structures involved in these transitions. For $1/\mathrm{Ro}_c$ it was well established that the new structure just beyond it consists of Ekman vortices which form near the plates, and the "order parameter" [1, 2] of the new phase was determined from direct numerical simulations (see Fig. 4 of Ref. [10]). Determining experimentally the changes of large-scale structures at $1/\mathrm{Ro}_{c,2}$ and $1/\mathrm{Ro}_{c,3}$ will be challenging. It can not be done in our apparatus where the extensive thermal shielding needed for the high-resolution (0.1% or better) heat-transport measurements reported in Figs. 1 and 5 prevents optical access. Perhaps it may be done more readily by DNS.

Possibly relevant to the symmetry of the structures is the formation of a Stewartson layer [34] as 1/Ro increases. Here it is interesting to note that the Stewartson-layer thickness reported in Refs. [34, 35] for $\Gamma = 1.00$ also suggests the existence of more than one transition as 1/Ro is increased. Structures at larger 1/Ro were reported for instance based on the numerical work of Ref. [36]. It is not clear how/whether these structures correlate with the experimentally observed transitions. But it is clear that the system can not evolve smoothly between structures that are vertically coherent over the sample height and are subject to a symmetry transformation about the horizontal mid plane on the one hand and structures that are vertically uncorrelated over the sample height (see *e.g.* Fig. 1 of Ref. [36]).

Finally one may ask whether our observation of a sequence of transitions is specific to finite systems with lateral boundaries. Although we do not know the answer for sure, we note that the structures of different symmetry reported in Ref. [36] are characteristic of the infinite system, and thus the unavoidably sharp transition between them will not depend on lateral boundaries. More globally, we call attention to the observation of cloud streets (see, for instance, Ref. [37]) in the laterally unbounded sky which undergo symmetry-breaking transitions [38], for instance due to the cross-roll instability, as "control parameters" (*i.e.* atmospheric conditions) change. These symmetry-breaking pattern changes also can not be smooth and must involve sharp transitions according to Landau's arguments.

This work was supported by NSF Grant DMR11-58514. SW acknowledges financial support by the Deutsche Forschungs Gesellschaft.

[1] L. Landau, Zh. Eksp. Teor. Fiz. **7**, 19 (1937).
[2] L. D. Landau, Phys. Z. Sowjet. **11**, 26 (1937).
[3] L. D. Landau, in *Collected papers of L.D. Landau*, edited by D. Ter-Haar (Oxford University Press, Oxford, 1965) pp. 193–216.
[4] A. Kolmogorov, Dokl. Akad. Nauk. SSSR. **30**, 299 (1941).
[5] S. Huisman, R. van der Veen, C. Sun, and D. Lohse, Nat. Commun. **5**, 1 (2014).
[6] F. Ravelet, L. Marié, A. Chiffaudel, and F. Daviaud, Phys. Rev. Lett. **93**, 164501 (2004).
[7] F. Ravelet, A. Chiffaudel, and F. Daviaud, J. Fluid Mech. **601**, 339 (2008).
[8] R. Stevens, J.-Q. Zhong, H. Clercx, G. Ahlers, and D. Lohse, Phys. Rev. Lett. **103**, 024503 (2009).
[9] P.-P. Cortet, A. Chiffaudel, F. Daviaud, and B. Dubrulle, Phys. Rev. Lett. **105**, 214501 (2010).
[10] S. Weiss, R. J. A. M. Stevens, J.-Q. Zhong, H. J. H. Clercx, D. Lohse, and G. Ahlers, Phys. Rev. Lett. **105**, 224501 (2010).
[11] S. Weiss and G. Ahlers, J. Fluid Mech. **684**, 407 (2011).
[12] L. P. Kadanoff, Phys. Today **54**, 34 (2001).
[13] G. Ahlers, Physics **2**, 74 (2009).
[14] G. Ahlers, S. Grossmann, and D. Lohse, Rev. Mod. Phys. **81**, 503 (2009).
[15] D. Lohse and K.-Q. Xia, Annu. Rev. Fluid Mech. **42**, 335 (2010).
[16] F. Chillà and J. Schumacher, Eur. Phys. J. E **35**, 58 (2012).
[17] M. V. R. Malkus, Proc. R. Soc. London A **225**, 196 (1954).
[18] C. H. B. Priestley, Aust. J. Phys. **7**, 176 (1954).
[19] C. H. B. Priestley, *Turbulent transfer in the lower atmosphere* (U. Chicago Press, Chicago, 1959).
[20] E. A. Spiegel, Ann. Rev. Astron. Astrophys. **9**, 323 (1971).
[21] J. Stevens, H. Clercx, and D. Lohse, E. J. Mech. B **40**, 41 (2013).
[22] H. T. Rossby, J. Fluid Mech. **36**, 309 (1969).
[23] K. Julien, S. Legg, J. McWilliams, and J. Werne, J. Fluid Mech. **322**, 243 (1996).
[24] J. E. Hart, Phys. Fluids **12**, 131 (2000).

[25] P. Vorobieff and R. E. Ecke, J. Fluid Mech. **458**, 191 (2002).
[26] P. Oresta, G. Stingano, and R. Verzicco, Eur. J. Mech. B **26**, 1 (2007).
[27] R. P. J. Kunnen, H. J. H. Clercx, and B. J. Geurts, Europhys. Lett. **84**, 24001 (2008).
[28] J.-Q. Zhong, R. Stevens, H. Clercx, R. Verzicco, D. Lohse, and G. Ahlers, Phys. Rev. Lett. **102**, 044502 (2009).
[29] R. J. A. M. Stevens, D. Lohse, and R. Verzicco, J. Fluid Mech. **688**, 31 (2011).
[30] J.-Q. Zhong and G. Ahlers, J. Fluid Mech. **665**, 300 (2010).
[31] S. Weiss and G. Ahlers, J. Fluid Mech. **676**, 1 (2011).
[32] P. Wei and G. Ahlers, J. Fluid Mech. **758**, 809 (2014).
[33] J. Niemela, S. Babuin, and K. Sreenivasan, J. Fluid Mech. **649**, 509 (2010).
[34] R. P. J. Kunnen, R. J. A. M. Stevens, J. Overkamp, C. Sun, G. F. van Heijst, and H. J. H. Clercx, J. Fluid Mech. **688**, 422 (2011).
[35] R. Kunnen, B. Geurts, and H. Clercx, J. Fluid Mech. **642**, 445 (2010).
[36] K. Julien, A. Rubio, I. Grooms, and E. Knobloch, Geophys. Astrophys. Fluid Dyn. **106**, 392 (2012).
[37] D. Etling and R. Brown, Boundary Layer Meteorology **65**, 215 (1993).
[38] F. H. Busse and R. M. Clever, J. Fluid Mech. **91**, 319 (1979).